



Statistical behavior of nonequilibrium and living biological systems subjected to active and thermal fluctuations

Ashesh Ghosh ¹ and Andrew J. Spakowitz ^{1,2,3,4,5,*}


¹*Department of Chemical Engineering, Stanford University, Stanford, California 94305, USA*

²*Department of Materials Science, Stanford University, Stanford, California 94305, USA*

³*Department of Chemistry, Stanford University, Stanford, California 94305, USA*

⁴*Department of Applied Physics, Stanford University, Stanford, California 94305, USA*

⁵*Biophysics Program, Stanford University, Stanford, California 94305, USA*

 (Received 26 June 2021; revised 12 October 2021; accepted 24 December 2021; published 25 January 2022)

We present a path-integral formulation of the motion of a particle subjected to fluctuating active and thermal forces. This general framework predicts the statistical behavior associated with the stochastic trajectories of the particle, accounting for all possible realizations of Brownian and active forces, over an arbitrary potential landscape. Temporal correlations in the active forces result in non-Markovian statistics, necessitating the inclusion of a fixed active-force value at specified times within the statistical treatment. We specialize our theory to that of exponentially correlated active forces for a particle in a harmonic potential. We find the exact results for the statistical distributions for the initial position of the particle, accounting for the impact of the correlated active forces at all times prior to the initial time. Our theory is then used to find the two-point distribution for the active Brownian particle, which governs the joint probability that a particle begins and ends at specified locations. Analyses of the active Brownian statistics demonstrate that the impact of active forces can be interpreted through a time-dependent temperature whose influence depends on the competition of timescales of the active-force correlation and the relaxation time of the particle in the harmonic potential. The general results presented in this work are transferable to a broad range of nonequilibrium systems with active and Brownian motion, and the time-dependent temperature serves as a governing principle to describe the competition of timescales associated with active forces and internal relaxation processes.

DOI: [10.1103/PhysRevE.105.014415](https://doi.org/10.1103/PhysRevE.105.014415)

I. INTRODUCTION

Active matter systems constantly harness energy (either from within the system or from its surroundings) to produce useful work or to enhance motion beyond that of Brownian diffusion alone [1–8]. Such systems are ubiquitous in nature. Examples of active forces at play work at varying length scales and timescales of dynamic phenomena including swarming bacterial cells or so-called “microswimmers” [9], artificially self-propelled Janus probes or “active” colloidal particles [10], ant colonies [11], schools of fish [12], flocking of birds [13], and correlated herd motion of animals [14].

Active forces also impact crucial biological processes at the microscale, such as enzymatic activity of proteins [15], gene expression in cells [16,17], the protein machinery that enables endosomal membrane fusion [18,19], biophysical properties of cell membranes [20–23], and cytoskeletal mechanical properties [24–26]. Large-scale dynamic rearrangement is central to chromosomal function as a repository of genetic information that must be stored, expressed, replicated, and divided. As with synthetic polymers [27], DNA in living cells undergoes stochastic motion that is characteristic of Brownian forces arising from thermal fluctuations.

However, numerous experimental observations indicate that “active” biological fluctuations play a central role in the motion of chromosomes in living cells [28–36]. Fundamental insight into the role of active biological fluctuations is essential to establishing a quantitative prediction of behavior in living cells.

Thermal fluctuations drive the stochastic Brownian motion of microscopic objects. The theoretical basis for predicting Brownian motion establishes a connection between the magnitude of Brownian forces from the thermal surroundings and the dissipation of heat from the friction exerted on the object [37,38]. The resulting fluctuation-dissipation theorem predicts stochastic trajectories whose time-averaged behavior is governed by equilibrium statistical thermodynamics. However, the introduction of active forces generally nullifies the use of the governing statistics from equilibrium statistical thermodynamics [39,40], although connections with equilibrium may exist in some limiting cases [41,42]. As such, it is necessary to establish a theoretical framework from which the statistical behavior of an active Brownian particle can be determined. Given the prevalence of nonequilibrium systems, this methodology would have a broad range of applications in the study of their dynamic behavior.

While the dynamics of a single particle in the presence of an arbitrary colored noise process is a long-studied problem [43–46], recent theoretical developments include efforts

*ajspakow@stanford.edu

towards understanding the nonequilibrium characterization of the system and thermodynamic irreversibility in the presence of active forces [2,7,47–52], motility-induced phase separation [42,53] and phase equilibrium [54], and generalized fluctuation relations for active matter systems [55,56]. These existing theoretical approaches primarily focus on a path-integral treatment based on the Onsager-Machlup integral and characterize the breaking of time-reversal symmetry with the introduction of active forces.

In this manuscript, we provide a path-integral formulation of the statistical behavior of particles that are acted on by both thermal (i.e., Brownian) and athermal active forces. Within our path-integral approach, we introduce a field transformation that enables the solution of the particle statistics in a range of problems. To account for the non-Markovian nature of active Brownian motion, we incorporate fixed values of the active force at specified times, allowing us to capture particle distributions with memory of all past active forces values. Specializing to the case of harmonic forces, we derive exact expressions for the initial and the two-point distributions, which are used to analyze the competition between the active-force timescale and the relaxation time of the particle in the harmonic potential. This competition is prevalent in active Brownian motion, and we introduce the concept of a time-dependent temperature to interpret the influence of active forces on relaxation processes with a given timescale.

II. PATH-INTEGRAL FORMULATION OF BROWNIAN MOTION WITH ACTIVE FORCES

We consider a particle undergoing random motion over a potential V . For our development, we focus on one-dimensional transport, but the final results are extended to three dimensions. The particle is subjected to a time-dependent fluctuating thermal force f_B (i.e., Brownian force) and an active force f_A that represents transient perturbations from the surrounding enzyme activity and, hence, is generically athermal in nature. The temporal evolution of the position $x(t)$ is governed by a modified Langevin equation,

$$\xi \frac{dx(t)}{dt} = f_V[x(t)] + f_B(t) + f_A(t), \quad (1)$$

where $f_V[x(t)] = -\frac{\partial V[x(t)]}{\partial x(t)}$ is the potential force on the particle at position x , and ξ is the friction constant of the medium.

The Brownian force f_B is governed by the fluctuation dissipation theorem, which states that f_B is a Gaussian-distributed random force that satisfies

$$\langle f_B(t) \rangle = 0, \quad (2)$$

$$\langle f_B(t)f_B(t') \rangle = \kappa^{(B)}(|t - t'|) = 2k_B T \xi \delta(t - t'). \quad (3)$$

This assumes that the environment is purely Newtonian, leading to the instantaneous decorrelation of Brownian forces (i.e., Gaussian white noise).

In our work, we additionally assume the active forces f_A are also stochastically varying with experimental conditions but still have well-defined statistical moments. Active forces

for our work are considered as also being Gaussian distributed with an arbitrary temporal correlation, such that

$$\langle f_A(t) \rangle = 0, \quad (4)$$

$$\langle f_A(t)f_A(t') \rangle = \kappa^{(A)}(|t - t'|), \quad (5)$$

where $\kappa^{(A)}(t)$ represents the temporal correlation between active forces (discussed in more detail below). In accordance with Doob's theorem [57], the athermal active colored noise Gaussian process corresponds to the Ornstein-Uhlenbeck (OU) process [58].

The short-time friction is completely oblivious to the existence of active forces in the system and, hence, the generalized fluctuation dissipation relation does not hold. Put another way, the existence of athermal active fluctuations modifies the effective conservative potential to a position- and time-dependent nonconservative one as $V_{\text{eff}}(t) = V[x(t)] - x(t)f_A(t)$, and the motion of the active Brownian particle is the same as the dynamics of a purely Brownian particle in the presence of a modified effective time-dependent potential.

We now frame the particle motion as a path-integral formulation, which recasts the Langevin equation [Eq. (1)] as a sum over particle trajectories. Since thermal fluctuations are Gaussian white noise, the probability can be written as

$$\begin{aligned} \mathcal{P}[f_B(t)] & \\ & \propto \exp \left[-\frac{1}{2} \int_0^t dt_1 \int_0^t dt_2 f_B(t_1) \kappa^{(B)-1}(|t_1 - t_2|) f_B(t_2) \right] \\ & = \exp \left\{ -\frac{1}{4k_B T \xi} \int_0^t dt_1 [f_B(t_1)]^2 \right\} \\ & = \int \mathcal{D}[w(t)] \exp \left\{ -k_B T \xi \int_0^t dt_1 [w(t_1)]^2 \right. \\ & \quad \left. - i \int_0^t dt_1 w(t_1) f_B(t_1) \right\}, \end{aligned} \quad (6)$$

where the last line introduces a Gaussian integral over a conjugate field $w(t)$. Since a random noise results in the dynamical variable randomly varying in time, we effectively write that the noise path tracks the dynamics of the particle itself. As the particle needs to follow the force-balance Langevin equation in the presence of active forces at each point in time, we write

$$\begin{aligned} \mathcal{P}[x(t)] & = \int \mathcal{D}[w(t)] \exp \left\{ -k_B T \xi \int_0^t dt_1 [w(t_1)]^2 \right. \\ & \quad \left. - i \int_0^t dt_1 w(t_1) [\xi \dot{x}(t_1) - f_V(x) - f_A(t_1)] \right\}, \end{aligned} \quad (7)$$

where the path probability is written for a specific realization of the active force $f_A(t_1)$.

Active forces exhibit temporal correlation, defined by the active-force correlation $\kappa^{(A)}(t)$. The particle statistics at any time hinges on the memory of past forces. Thus, the statistical distribution for the particle depends both on the current position and the current active force, necessitating the inclusion of a fixed active force at a given time within the statistical treatment. To do this, we define a fixed time $t = t_0$ where the magnitude of the active force is given by $f_A^{(0)}$. Hence, for any

given path of the particle from $x(t=0) = x_0$ to $x(t) = x$ for the given fixed value of active force $f_A^{(0)}$ at $t = t_0$, we write

$$\begin{aligned} \mathcal{P}[x|x_0; t, t_0] &= \int_{x_0}^x \mathcal{D}[x(t)] \int \mathcal{D}[w(t)] \int \mathcal{D}[f_A(t)] \\ &\times \exp \left\{ -k_B T \xi \int_0^t dt_1 [w(t_1)]^2 \right. \\ &\quad \left. - i \int_0^t dt_1 w(t_1) [\xi \dot{x}(t_1) - f_V[x(t_1)] - f_A(t_1)] \right\} \\ &\times \mathcal{P}[f_A(t)] \delta(f_A(t_0) - f_A^{(0)}), \end{aligned} \quad (8)$$

where $\mathcal{P}[f_A]$ is the probability density functional of the active noise. We write the δ function using a Fourier representation to result in the expression

$$\begin{aligned} \mathcal{P}[x|x_0; t, t_0] &= \int_{x_0}^x \mathcal{D}[x(t)] \int \mathcal{D}[w(t)] \int \mathcal{D}[f_A(t)] \int d\eta \\ &\times \exp \left\{ -k_B T \xi \int_0^t dt_1 [w(t_1)]^2 \right. \\ &\quad \left. + i \xi \int_0^t dt_1 \dot{w}(t_1) x(t_1) - i \xi w(t) x(t) + i \xi w(0) x(0) \right. \\ &\quad \left. + i \int_0^t dt_1 w(t_1) [f_V[x(t_1)] + f_A(t_1)] \right. \\ &\quad \left. + i \eta \int_0^t dt_1 \delta(t_1 - t_0) f_A(t_1) - i \eta f_A^{(0)} \right\} \mathcal{P}[f_A(t)]. \end{aligned} \quad (9)$$

We perform the integral over the active forces by noting a Gaussian form of active forces,

$$\begin{aligned} \mathcal{P}[f_A(t)] &\propto \exp \left[-\frac{1}{2} \int_0^t dt_1 \int_0^t dt_2 f_A(t_1) \kappa^{(A)-1}(|t_1 - t_2|) f_A(t_2) \right], \end{aligned} \quad (10)$$

which results in the expression

$$\begin{aligned} \mathcal{P}[x|x_0; t, t_0] &= \int_{x_0}^x \mathcal{D}[x(t)] \int \mathcal{D}[w(t)] \int d\eta \\ &\times \exp \left\{ -k_B T \xi \int_0^t dt_1 [w(t_1)]^2 dt_1 + i \xi \int_0^t dt_1 \dot{w}(t_1) x(t_1) \right. \\ &\quad \left. - i \xi w(t) x(t) + i \xi w(0) x(0) + i \int_0^t dt_1 w(t_1) f_V[x(t_1)] \right. \\ &\quad \left. - \frac{1}{2} \int_0^t dt_1 \int_0^t dt_2 w(t_1) \kappa^{(A)}(|t_1 - t_2|) w(t_2) - i \eta f_A^{(0)} \right. \\ &\quad \left. - \eta \int_0^t dt_1 \kappa^{(A)}(|t_1 - t_0|) w(t_1) - \frac{1}{2} \eta^2 \kappa^{(A)}(0) \right\}. \end{aligned} \quad (11)$$

Our development is currently one-dimensional. Extending this approach to three dimensions (or arbitrary dimensions) requires us to translate from one-dimensional scalar variables to vector representations, such that $x \rightarrow \vec{r}$, $w \rightarrow \vec{w}$, $\eta \rightarrow \vec{\eta}$, and

$f_A^{(0)} \rightarrow \vec{f}_A^{(0)}$. With these modifications, we write the general expression as

$$\begin{aligned} \mathcal{P}[\vec{r}|\vec{r}_0; t, t_0] &= \int_{\vec{r}_0}^{\vec{r}} \mathcal{D}[\vec{r}(t)] \int \mathcal{D}[\vec{w}(t)] \int d\vec{\eta} \\ &\times \exp \left\{ -k_B T \xi \int_0^t dt_1 [\vec{w}(t_1)]^2 + i \xi \int_0^t dt_1 \dot{\vec{w}}(t_1) \cdot \vec{r}(t_1) \right. \\ &\quad \left. - i \xi \vec{w}(t) \cdot \vec{r}(t) + i \xi \vec{w}(0) \cdot \vec{r}(0) \right. \\ &\quad \left. + i \int_0^t dt_1 \vec{w}(t_1) \cdot \vec{f}_V[\vec{r}(t_1)] \right. \\ &\quad \left. - \frac{1}{2} \int_0^t dt_1 \int_0^t dt_2 \kappa^{(A)}(|t_1 - t_2|) \vec{w}(t_1) \cdot \vec{w}(t_2) - i \vec{\eta} \cdot \vec{f}_A^{(0)} \right. \\ &\quad \left. - \int_0^t dt_1 \kappa^{(A)}(|t_1 - t_0|) \vec{\eta} \cdot \vec{w}(t_1) - \frac{1}{2} \vec{\eta}^2 \kappa^{(A)}(0) \right\}. \end{aligned} \quad (12)$$

While our subsequent analyses focus on one-dimensional transport, the conclusions and approaches presented here are amenable to analysis of behavior of arbitrary dimensions.

The current form for the joint probability $\mathcal{P}[x|x_0; t, t_0]$ adopts a convenient form for our subsequent analyses. However, it is illustrative to consider the case where we integrate over $w(t)$ and $f_A^{(0)}$. Performing these Gaussian integrals, we arrive at the expression

$$\begin{aligned} \mathcal{P}[x|x_0; t] &= \int_{x_0}^x \mathcal{D}[x(t)] \\ &\times \exp \left(-\frac{1}{2} \int_0^t dt_1 \int_0^t dt_2 \{ \xi \dot{x}(t_1) - f_V[x(t_1)] \} \right. \\ &\quad \left. \times \kappa^{(AB)-1}(|t_1 - t_2|) \{ \xi \dot{x}(t_2) - f_V[x(t_2)] \} \right). \end{aligned} \quad (13)$$

While the above equation can be intuitively written as a result of underlying Gaussian processes (both white and colored noise), the preceding derivation would be instructive to obtain the conditional probability distribution as a function of any specific realization of $\vec{f}_A^{(0)}$, which we exploit in our subsequent analyses. The active Brownian kernel $\kappa^{(AB)}(t_1 - t_2) = 2k_B T \xi \delta(t_1 - t_2) + \kappa^{(A)}(t_1 - t_2)$ gives the combined force correlation for active and Brownian forces, and the kernel inverse function $\kappa^{(AB)-1}$ satisfies

$$\int_{-\infty}^{\infty} dt_2 \kappa^{(AB)}(t_1 - t_2) \kappa^{(AB)-1}(t_2 - t_3) = \delta(t_1 - t_3). \quad (14)$$

We perform a Fourier transform from $t_1 - t_3$ to the frequency ω , resulting in the Fourier-transformed representation

$$\tilde{\kappa}^{(AB)-1}(\omega) = \frac{1}{\tilde{\kappa}_{AB}(\omega)} = \frac{1}{2k_B T \xi + \tilde{\kappa}_A(\omega)}. \quad (15)$$

This form suggests the stochastic motion exhibits a frequency (i.e., time) dependence for the weighting of the fluctuating paths. In this regard, the particle experiences an effective temperature that depends on the timescale of observation or the relaxation timescale of the potential. This time-dependent temperature is valuable in interpreting the impact of active forces on dynamic processes (discussed further below).

Our theoretical development so far is general to any form of the spatially varying potential $V(x)$ and does not assume any special form for the active-force correlation. We specialize to the case of the harmonic potential for further analysis and discussion.

III. ACTIVE BROWNIAN PARTICLE IN A HARMONIC POTENTIAL

Here, we specialize to the case of the harmonic potential $V(x) = \frac{1}{2}kx^2$ and the potential force $f_V[x(t)] = -kx(t)$, where k is the force constant. The quantities x , t , and f are made nondimensional by $x_0 = \sqrt{k_B T/k}$, $t_0 = x_0^2 \xi / (k_B T)$, and $f_0 = k_B T / x_0 = \sqrt{k_B T k}$, respectively. This results in the dimensionless variables $u = x/x_0$, $\tau = t/t_0$, and $F = f/f_0$.

The path integral over position variable $u(\tau)$ is carried out, resulting in a δ functional over the conjugate field, such that

$$\begin{aligned} \mathcal{P}[u|u_0; \tau, \tau_0] &= \int \mathcal{D}[w(t)] \int d\eta \exp \left\{ - \int_0^\tau d\tau_1 [w(\tau_1)]^2 \right. \\ &\quad - iw(\tau)u + iw(0)u_0 - i\eta F_A^{(0)} \\ &\quad - \frac{1}{2} \int_0^\tau d\tau_1 \int_0^\tau d\tau_2 w(\tau_1) \kappa^{(A)}(|\tau_1 - \tau_2|) w(\tau_2) \\ &\quad \left. - \eta \int_0^\tau d\tau_1 \kappa^{(A)}(|\tau_1 - \tau_0|) w(\tau_1) - \frac{1}{2} \eta^2 \kappa^{(A)}(0) \right\} \\ &\quad \times \prod_\tau \delta[\dot{w}(\tau) - w(\tau)]. \end{aligned} \quad (16)$$

The δ functional over the conjugate field w results in the condition $\dot{w}(\tau) = w(\tau)$. Therefore, we write $w(\tau_1) = w(\tau) \exp[-(\tau - \tau_1)] = W \exp[-(\tau - \tau_1)]$ for any arbitrary

time $\tau_1 < \tau$. For the OU process, we have

$$\begin{aligned} \kappa^{(A)}(|\tau_1 - \tau_2|) &= \langle F_A(\tau_1) F_A(\tau_2) \rangle \\ &= F_A^2 \exp(-K_A |\tau_1 - \tau_2|), \end{aligned} \quad (17)$$

where F_A^2 defines the strength of active drive, and $K_A = \tau_B / \tau_A$ is the dimensionless rate of active force relaxation.

The argument of the exponential of Eq. (16) can now be evaluated based on the functional form of $w(\tau)$. We first evaluate the following term:

$$-\eta \int_0^\tau d\tau_1 \kappa^{(A)}(|\tau_1 - \tau_0|) w(\tau_1) = -F_A^2 \eta W G_A(\tau, \tau_0), \quad (18)$$

where

$$\begin{aligned} G_A(\tau, \tau_0) &= \frac{1}{K_A + 1} (e^{-\tau + \tau_0} - e^{-K_A \tau_0 - \tau}) \\ &\quad + \frac{1}{K_A - 1} (e^{-\tau + \tau_0} - e^{-K_A \tau + K_A \tau_0}). \end{aligned} \quad (19)$$

We now write Eq. (16) as

$$\begin{aligned} \mathcal{P}[u|u_0; \tau, \tau_0] &= \int_{-\infty}^\infty dW \int_{-\infty}^\infty d\eta \\ &\quad \times \exp \left\{ - \frac{W^2}{2} [1 - e^{-2\tau} + F_A^2 H_A(\tau)] \right. \\ &\quad - iW(u - u_0 e^{-\tau}) - F_A^2 G_A(\tau, \tau_0) \eta W \\ &\quad \left. - \frac{1}{2} \eta^2 F_A^2 - i\eta F_A^{(0)} \right\}, \end{aligned} \quad (20)$$

where

$$H_A(\tau) = \frac{1}{1 - K_A^2} [(1 + e^{-2\tau}) - K_A(1 - e^{-2\tau}) - 2e^{-(1+K_A)\tau}]. \quad (21)$$

Integrating over the η and W variables, we arrive at

$$\mathcal{P}[u|u_0; \tau, \tau_0] = \frac{1}{\mathcal{N}} \exp \left\{ - \frac{(u - u_0 \exp(-\tau) - G_A(\tau, \tau_0) F_A^{(0)})^2}{2\{1 - \exp(-2\tau) + F_A^2 [H_A(\tau) - G_A(\tau, \tau_0)^2]\}} - \frac{(F_A^{(0)})^2}{2F_A^2} \right\}, \quad (22)$$

where the normalization constant \mathcal{N} follows from

$$\int_{-\infty}^\infty du \int_{-\infty}^\infty dF_A^{(0)} \mathcal{P}[u|u_0; \tau, \tau_0] = 1. \quad (23)$$

This results in the expression

$$\mathcal{N} = 2\pi F_A \sqrt{1 - \exp(-2\tau) + F_A^2 [H_A(\tau) - G_A(\tau, \tau_0)^2]}. \quad (24)$$

The probability $\mathcal{P}[u|u_0; \tau, \tau_0]$ provides the joint probability that a particle with position u_0 at time $\tau = 0$ is located at position u at time τ given that there is a force $F_A^{(0)}$ at time τ_0 . To help interpret this, we consider a particle that is located at u_0 and is subjected to the force $F_A^{(0)} = 10$ at the initial time $\tau_0 = 0$ with the average active-force magnitude $F_A = 10$ (i.e., $F_A^{(0)} = F_A = 10$). While it should be noted that there is no knowledge available on the specific realization of $F_A^{(0)} = 10$ or any particular value of $F_A^{(0)}$ for that matter in any real system,

use of $F_A^{(0)}$ properly accounts for the history-dependent force the system feels at $\tau = \tau_0$. Eventually the distribution has to be accounted for by integrating over all possible realizations of the initial force $F_A^{(0)}$. Here, our choice $F_A^{(0)} = 10$ has been used to illustrate the effects on the dynamical properties of the system for a particular such realization. We define the most likely position $u^* = u_0 \exp(-\tau) + G_A(\tau, \tau_0) F_A^{(0)}$, which gives the position with the highest probability \mathcal{P} . For the conditions under consideration, we have $u^* = G_A(\tau, \tau_0) = 0$, demonstrating that G_A dictates the trajectory of a particle at time τ given the active force $F_A^{(0)}$ at τ_0 . This accounts for the initial active motion, since $G_A \approx \tau$ for short times τ (note, $\tau_0 = 0$), and the eventual decay to 0 for times $\tau \gg 1/K_A$ relates to the eventual loss of correlation of the active forces. The top plot of Fig. 1 shows the most likely position $u^*/F_A^{(0)}$ for the current conditions ($u_0 = 0$ and $F_A^{(0)} = 1$ at $\tau_0 = 0$) for varying values of K_A from $K_A = 10^0$ to $K_A = 10^{-5}$. As $K_A \rightarrow 0$, the most likely position follows the athermal

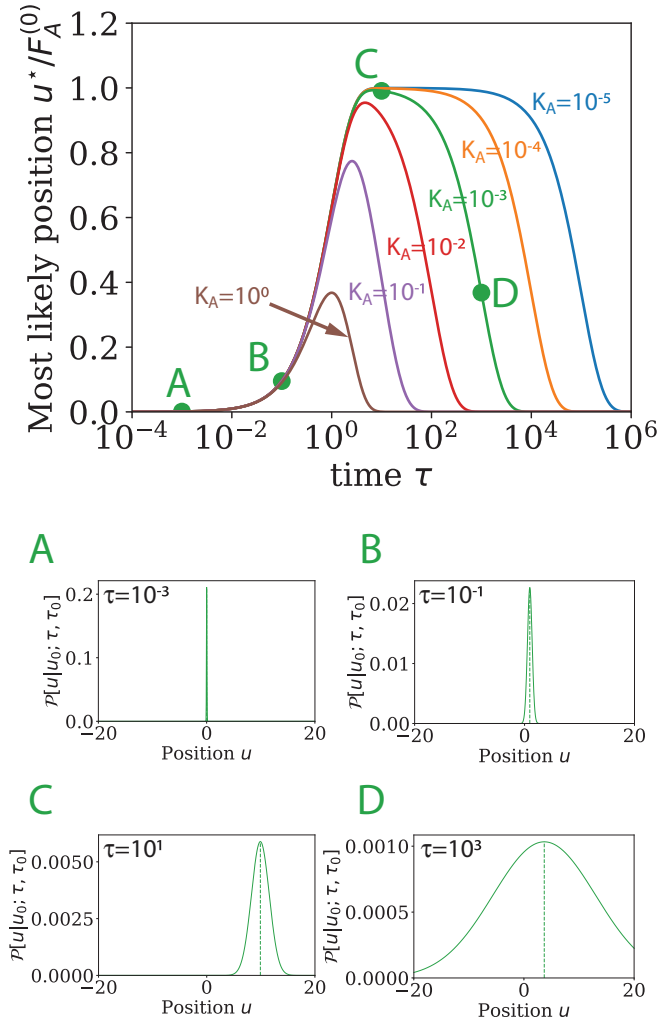


FIG. 1. Top plot shows the most likely position $u^*/F_A^{(0)}$ versus time τ for a particle that begins at position $u_0 = 0$ subject to an initial active force $F_A^{(0)} = 10$ for varying active-force rate constants ranging from $K_A = 10^{-5}$ to $K_A = 10^0$. The average active-force magnitude is $F_A = 10$, such that $F_A^{(0)} = 10$ is within the typical range of values. The bottom plots show the probability $\mathcal{P}[u|u_0; \tau, \tau_0]$ versus u for four times ranging from $\tau = 10^{-3}$ to $\tau = 10^3$ for $K_A = 10^{-3}$, as labeled as A, B, C, and D in the top plot.

trajectory $u^*/F_A^{(0)} \rightarrow 1 - e^{-\tau}$, reflecting the lack of decorrelation of the active force F_A .

Our dimensionless time $\tau = t/t_0$ gives the time relative to the relaxation time of the particle in the harmonic potential. For the active-force time $\tau_A = 1/K_A \gg 1$, the intermediate timescale of observation ($1 < \tau < \tau_A$) results in the most likely position $u^* \approx 1$. This regime is followed by a precipitous drop to $u^* \rightarrow 0$ at later times $\tau \gg \tau_A$ as the active forces lose correlation. As $\tau_A \rightarrow 1$, the particle is unable to reach $u^* \approx 1$ prior to loss of correlation in the active force, resulting in a u^* that cannot reach $u^* \approx 1$ prior to dropping to 0 (e.g., $K_A = 10^0$ curve in the top plot of Fig. 1).

The bottom plot of Fig. 1 shows the probability distribution $\mathcal{P}[u|u_0; \tau, \tau_0]$ at four time points $\tau = 10^{-3}$, 10^{-1} , 10^1 , and 10^3 for $K_A = 10^{-3}$ (labeled A, B, C, and D in the top plot of Fig. 1). These plots show the nonmonotonic behavior of the

most likely position u^* , and the variance of these distributions progressively increases with time. At short times ($\tau \ll 1$), the variance increases from 0 to 1, which is the thermal variance (i.e., independent of active forces). At intermediate times ($1 < \tau \ll \tau_A$), there is a plateau in the variance at 1 until the active forces decorrelate as $\tau \rightarrow \tau_A$. Thereafter, the variance increases to a value $1 + F_A^2/(1 + K_A)$ as $\tau \rightarrow \infty$. This progression of behaviors is specific to a large separation in timescales, such that $\tau_A \gg 1$. Conditions where $\tau_A \lesssim 1$ leads to a monotonic increase in the variance to $1 + F_A^2/(1 + K_A)$ without an intermediate plateau.

Our inclusion of the fixed force $F_A^{(0)}$ is critical in resolving the appropriate distribution of initial positions u_0 . This initial distribution must account for the memory of the active forces at all times prior to the initial time (i.e., all times from $-\infty$ to $\tau_0 = 0$). Alternatively, we shift the fixed-force time to the end time ($\tau_0 = \tau$) and take the limit as time approaches ∞ , resulting in a stable distribution that represents the temporal memory of all correlated active forces. This leads to the initial distribution

$$\begin{aligned} \mathcal{P}_0(u_0) &= \lim_{\tau \rightarrow \infty} \mathcal{P}[u_0|u_{-\infty}; \tau, \tau_0 = \tau] \\ &= \frac{1}{\mathcal{N}} \exp \left\{ -\frac{[u_0 - F_A^{(0)}/(1 + K_A)]^2}{2[1 + F_A^2 K_A/(1 + K_A)]} - \frac{(F_A^{(0)})^2}{2F_A^2} \right\}. \end{aligned} \quad (25)$$

The normalization constant \mathcal{N} is found to be $\mathcal{N} = 2\pi F_A [1 + F_A^2 K_A/(1 + K_A)]^{1/2}$.

We define the most likely initial position $u_0^* = F_A^{(0)}/(1 + K_A)$, which gives the position of the maximum probability $\mathcal{P}_0(u_0)$, and the position variance in the initial distribution $\sigma_0^2 = 1 + F_A^2 K_A/(1 + K_A)^2$. The top plot of Fig. 2 shows the properties of the initial distribution $\mathcal{P}_0(u_0)$ by plotting the most likely position $u_0^*/F_A^{(0)}$ and the variance $\sqrt{\sigma_0^2 - 1}/F_A$ versus K_A . The bottom plots in Fig. 2 show $\mathcal{P}_0(u_0)$ versus the initial position u_0 for the four values of K_A identified in the top plot ($F_A = F_A^{(0)} = 10$).

The most likely position exhibits a plateau value $u_0^*/F_A^{(0)} \rightarrow 1$ as $K_A \rightarrow 0$. For small values of K_A , the active force remains correlated for sufficient time for the particle to reach its preferred position $u_0 = F_A^{(0)}$ during the time period prior to arriving at u_0 at time 0 (i.e., $\tau \in (-\infty, 0]$). As K_A increases, the particle experiences a shorter time of correlated active forces, and the particle is unable to reach its preferred position. The crossover between these regimes is $\tau_A = 1$, since this marks the point where the active-force correlation time is equal to the relaxation time of the particle in the harmonic potential.

The variance exhibits a nonmonotonic behavior with a maximum value at $K_A = 1$. For small values $K_A \ll 1$, the particle is able to reach its preferred position $u_0 = F_A^{(0)}$, and the variance is associated with thermal fluctuations around this preferred position. This results in the limiting behavior $\sigma_0^2 \rightarrow 1$ as $K_A \rightarrow 0$. For large values $K_A \gg 1$, the active forces decorrelate rapidly, much in the manner of thermal fluctuations. Decorrelation occurs at timescales that are much shorter than relaxation within the harmonic potential, and the particle cannot distinguish between thermal fluctuations and active

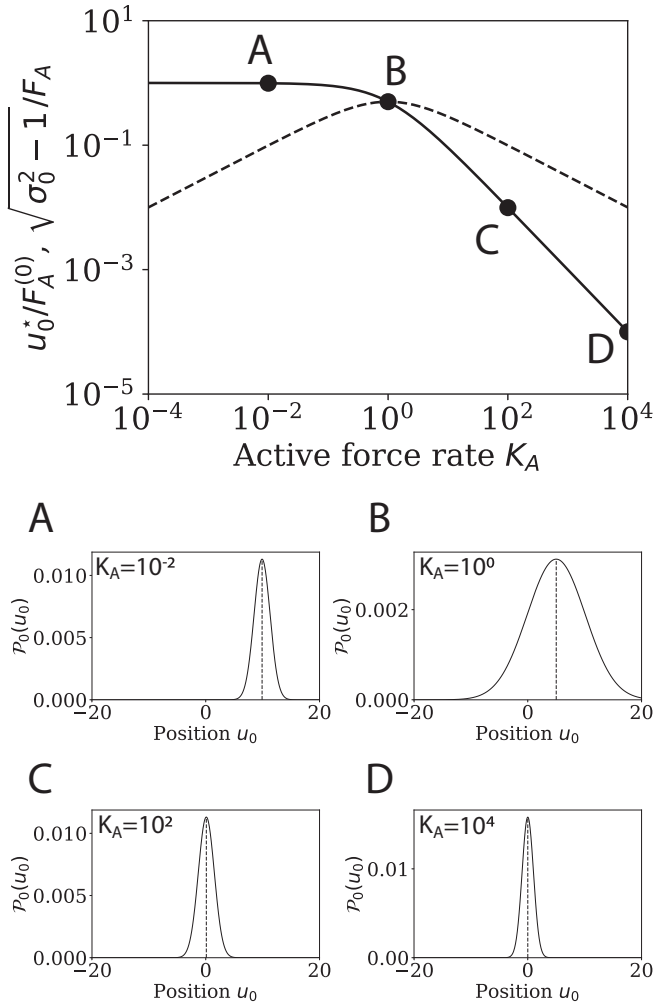


FIG. 2. The top plot shows the most likely position $u_0^*/F_A^{(0)}$ and the variance $\sqrt{\sigma_0^2 - 1/F_A}$ for the initial-position distribution $\mathcal{P}_0(u_0)$ over a range of active-force rates K_A . The bottom plots show $\mathcal{P}_0(u_0)$ versus u_0 for the four values $K_A = 10^{-2}, 10^0, 10^2,$ and 10^4 identified in the top plot.

fluctuations. In this regime, it is useful to define an effective active temperature $\Gamma = F_A^2/K_A$ that reflects how the active forces contribute to the fluctuations within the harmonic trap. This leads to the initial variance $\sigma_0^2 = 1 + \Gamma K_A^2/(1 + K_A)^2$, which saturates to $\sigma_0^2 \rightarrow 1 + \Gamma$ as $K_A \rightarrow \infty$.

This leads to a picture where the particle exhibits two regimes of behavior. For $K_A \ll 1$, the particle tracks with the preferred position $u_0 = F_A^{(0)}$ when the timescale of relaxation in the harmonic well is much shorter than τ_A , and the variance is dictated by thermal fluctuations around this preferred position. For $K_A \gg 1$, the particle experiences random active fluctuations that are indistinguishable from thermal fluctuations, resulting in an initial distribution that is centered at 0 with the effective active Brownian temperature $T_{AB}^{\text{eff}} = 1 + \Gamma$.

We now have the ingredients to define a two-point distribution, $P_2(u|u_0; \tau)$. This distribution captures the joint probability that a particle that is located at position u_0 at time 0 is located at u at time τ , integrated over the active force at time 0. Based on this definition, the two-point distribution is

given by

$$P_2(u|u_0; \tau) = \int_{-\infty}^{\infty} dF_A^{(0)} \mathcal{P}(u|u_0; \tau, \tau_0 = 0) \mathcal{P}_0(u_0). \quad (26)$$

The solution of the two-point distribution is rendered as a Fourier transform (from u to k and u_0 to k_0) to be

$$\tilde{P}_2(k|k_0; \tau) = \exp\left[-\frac{1}{2}\left(1 + \frac{F_A^2}{1+K_A}\right)(k^2 + k_0^2) - C_u(\tau)kk_0\right], \quad (27)$$

where we define the position correlation function

$$C_u(\tau) = \langle u(\tau)u(0) \rangle = e^{-\tau} + \frac{F_A^2}{K_A^2 - 1}(K_A e^{-\tau} - e^{-K_A \tau}). \quad (28)$$

The tilde on the two-point distribution indicates the Fourier transform from u to k and from u_0 to k_0 .

Upon Fourier inversion, we find the two-point distribution to be

$$P_2(u|u_0; \tau) = \frac{1}{\mathcal{N}} \exp\left\{-\frac{C_u(0)(u^2 + u_0^2) - 2C_u(\tau)uu_0}{2[C_u(0)^2 - C_u(\tau)^2]}\right\}, \quad (29)$$

where $C_u(0) = \lim_{\tau \rightarrow 0} C_u(\tau) = 1 + F_A^2/(1 + K_A)$.

The two-point distribution P_2 gives the joint probability after integrating over the initial force $F_A^{(0)}$, accounting for the appropriate initial distributions \mathcal{P}_0 from all active forces before $\tau = 0$. The resulting distribution is symmetric in u and u_0 , with a temporal correlation that only depends on the position correlation function $C_u(\tau) = \langle u(\tau)u(0) \rangle$. Decorrelation of the position arises from two contributions: relaxation of the particle within the harmonic potential (at timescale $\tau \approx 1$) and decorrelation of the most likely position u^* (at timescale $\tau \approx \tau_A$). The integration over $F_A^{(0)}$ causes these two contributions to be convolved within C_u , and their independent contributions can be inferred from the temporal relaxation of C_u .

Figure 3 shows the position correlation function C_u versus time τ for varying active-force rate constants K_A from 10^1 to 10^{-4} and the active-force magnitude $F_A = 1$. Here, we choose $F_A = 1$ to have equal weighting from potential-force relaxation and active-force relaxation in C_u . For short active-force times $\tau_A = 1/K_A \ll 1$, the position relaxation at time $\tau \approx 1$ dominates the behavior. These conditions coincide with the active forces behaving as an effective temperature, leading to the form $C_u \rightarrow (1 + \Gamma)e^{-\tau}$ as $K_A \rightarrow \infty$.

For long active-force times $\tau_A \gg 1$ (i.e., $K_A \ll 1$), position decorrelation occurs in two distinct stages. First, the particle relaxes within its local harmonic potential at time $\tau \approx 1$, followed by a plateau in C_u before a terminal relaxation to 0 at time $\tau \approx \tau_A$. The potential center remains correlated during the intermediate timescale $1 \ll \tau \ll \tau_A$, and the subsequent relaxation occurs as the active force decorrelates. An alternative picture is that the active force itself is a diffusing quantity with a relaxation time for its diffusive motion of τ_A . The intermediate- and long-time behavior represents the contribution of the active-force relaxation processes, which are much slower than the particle relaxation for $K_A \ll 1$.

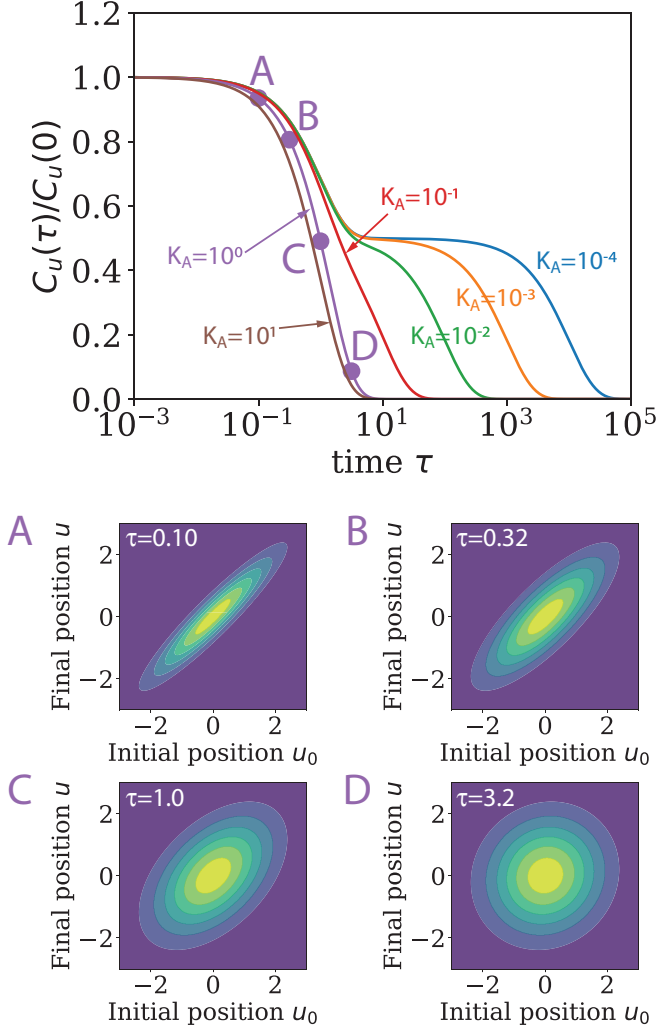


FIG. 3. The top plot shows the normalized position correlation function $C_u(\tau)/C_u(0)$ versus time τ for $F_A = 1$ and $K_A = 10^{-4}$ to $K_A = 10^1$. The four time points labeled A to D for the $K_A = 10^0$ curve coincide with values associated with the bottom plots of the two-point distributions $P_2(u|u_0; \tau)$.

The bottom plots in Fig. 3 show surface plots of the two-point function $P_2(u|u_0; \tau)$ at the four times τ labeled in the top plot for $K_A = 1$. These plots demonstrate the behavior as the position correlation function relaxes to 0. Short times (e.g., $\tau = 0.10$ in Fig. 3) result in considerable correlation between the initial and final positions, resulting in a probability distribution that is peaked around $u = u_0$. As $C_u \rightarrow 0$ with increasing time, the two-point function exhibits a spreading along the axis orthogonal to the line $u = u_0$, demonstrating the eventual loss of correlation. The symmetric probability distribution as $\tau \rightarrow \infty$ reflects the limiting form $P_2(u|u_0; \tau \rightarrow \infty) = P_0(u)P_0(u_0)$, where

$$P_0(u) = \int_{-\infty}^{\infty} dF_A^{(0)} \mathcal{P}_0(u) = \frac{1}{\mathcal{N}} \exp\left\{-\frac{u^2}{2[1 + F_A^2/(1 + K_A)]}\right\}. \quad (30)$$

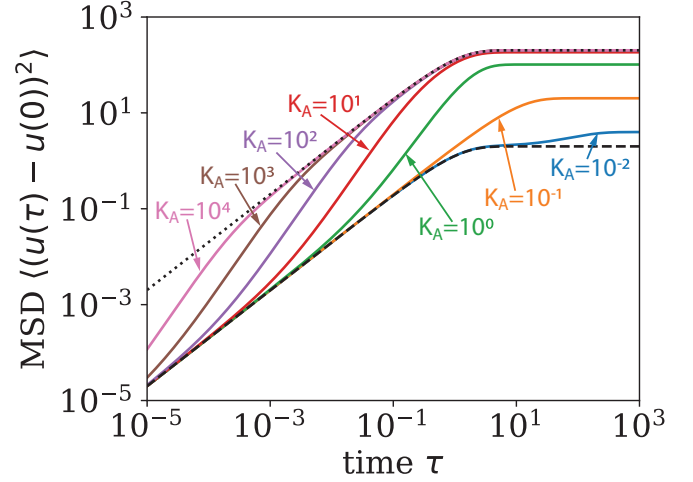


FIG. 4. Plot of the mean-square displacement (MSD) versus time τ for $\Gamma = F_A^2/K_A = 100$ and a range of active-force rates $K_A = 10^{-2}$ to $K_A = 10^4$ (as labeled in the plot).

This Gaussian distribution arises from the combination of Brownian fluctuations and active forces contributing to the variance $1 + F_A^2/(1 + K_A) = 1 + \Gamma K_A/(1 + K_A)$, which tends to $1 + \Gamma$ in the limit $K_A \rightarrow \infty$. The limiting behavior indicates the statistically independent nature of the probability distribution in the long-time limit.

The mean-squared displacement (MSD) is determined from the position correlation function to be

$$\begin{aligned} MSD(\tau) &= \langle [u(\tau) - u(0)]^2 \rangle = 2[C_u(0) - C_u(\tau)] \\ &= 2(1 - e^{-\tau}) + \frac{2F_A^2}{K_A^2 - 1} [K_A(1 - e^{-\tau}) - (1 - e^{-K_A\tau})]. \end{aligned} \quad (31)$$

In Fig. 4, we plot the MSD versus time τ over a range of active-force rates from $K_A = 10^{-2}$ to $K_A = 10^4$ (as labeled in the plot) for a fixed active-force temperature $\Gamma = 100$. We include the Brownian-only mean-square displacement $MSD_B = 2(1 - e^{-\tau})$ as the dashed curve. We define the active Brownian mean-square displacement $MSD_{AB} = 2(1 + \Gamma)(1 - e^{-\tau})$ (dotted curve in Fig. 4). This gives the limiting behavior under conditions where the active forces act as effective thermal fluctuations ($K_A \rightarrow \infty$).

The mean-square displacement exhibits an initial Brownian diffusion $MSD \approx 2\tau$ for times $\tau \ll \tau_A = 1/K_A$. For cases where $\tau_A \ll 1$, the MSD exhibits an enhanced transport to an effective active Brownian diffusion $MSD \approx 2(1 + \Gamma)\tau$ for $\tau_A \ll \tau \ll 1$, prior to reaching the terminal plateau value of $MSD \rightarrow 2(1 + \Gamma)$ for $\tau \gg 1$. Conditions where $\tau_A \gg 1$ (i.e., $K_A \ll 1$) lead to the particle reaching the Brownian plateau $MSD \approx 2$ prior to the active-force decorrelation, leading to a temporary plateau prior to elevating to the active Brownian plateau $MSD \rightarrow 2[1 + \Gamma K_A/(1 + K_A)]$ for $\tau \gg \tau_A$ (see the $K_A = 10^{-2}$ curve in Fig. 4).

Our development of a path-integral representation of active Brownian motion provides the full statistical description of particle motion in the presence of correlated active forces. If one cares only about obtaining the position correlation or the

MSD in the presence of active forces, we note an alternative route is possible, as sketched in Appendix A.

We find that $C_u(\tau)$ follows the differential equation

$$\frac{dC_u(\tau)}{d\tau} = -C_u(\tau) + \frac{F_A^2}{K_A + 1} \exp(-K_A \tau). \quad (32)$$

In the limit $F_A \rightarrow 0$, the above equation reduces to the differential equation for a simple exponential relaxation $\frac{dC_u(\tau)}{d\tau} = -C_u(\tau)$ followed by pure Brownian particles in the absence of active forces.

In all the results presented in this work, the timescale of relaxation of the particle or effective dynamics can be explained in terms of the higher effective temperature of the system, albeit sometimes time dependent. But this becomes complicated for a system with a spectrum of relaxation timescales, where some relaxation processes are faster or slower than the active-force correlation time. Such effects are prevalent for the dynamics of a polymer chain subjected to both active and Brownian fluctuations, as we explore in the accompanying article [59].

IV. CONCLUSIONS

In this paper, we study the dynamics of a particle in the presence of both active and Brownian fluctuations. We develop a general framework for predicting the statistical behavior of the active-Brownian particle based on a path-integral approach. The active forces are assumed to be Gaussian distributed with an arbitrary temporal correlation whose functional form dictates how the active forces communicate in time. This active-force memory necessitates the inclusion of the initial active force within the particle statistics, and our approach appropriately incorporates these correlations in a manner that acknowledges the non-Markovian nature of the statistical behavior. Within this approach, we introduce a field transformation that facilitates the solution of the particle statistics, which typically exhibit non-Markovian properties and are not easily formulated as a diffusion equation. We show within this framework that the active Brownian particle is driven by a frequency-dependent (or time-dependent) “temperature” that impacts the particle dynamics based on the timescale of relaxation of the system. It should be noted that time-dependent temperature can only be defined in a heuristic way by *ad hoc* invoking equipartition theorem at all timescales and not from a true equilibrium thermodynamic state of the system. Our current approach is based on a path-integral formalism that tracks only the position of the particle and has been shown to be insufficient in capturing the entropy production aspects of a Brownian particle in the presence of active noise [49]. However, this limitation does not alter the position distribution that integrates out fluctuating active forces or the mean-squared displacement of the particle that feels only the averaged-out time-dependent nature of the active forces.

We then proceed to analyze the active Brownian motion of a particle in a harmonic potential. This potential has a single characteristic timescale of relaxation and thus serves to illustrate the impact of a time-dependent temperature on particle dynamics. In the case of exponentially correlated

active forces (i.e., with a single characteristic timescale), our theory predicts a competition between the active-force timescale and the relaxation time in the harmonic potential. The initial distribution of particle positions for a given initial active force retains memory from the correlated active forces prior to time 0. However, this effect only arises when the active-force timescale exceeds that of relaxation within the harmonic potential. The position correlation after the initial time exhibits relaxation based on two contributions: relaxation within the harmonic potential and decorrelation of the active forces. However, these two contributions can only be distinguished when the active-force time is much larger than the harmonic-relaxation time.

We show that the mean-square displacement (MSD) for an active Brownian particle in a harmonic potential exhibits a distinct transition in behavior from short to long times. The early-time MSD (i.e., times much shorter than the active-force time) is diffusive with a characteristic temperature T that coincides with the thermal temperature. At long times, the MSD exhibits a progression to a plateau value that is dictated by the effective active Brownian temperature T_{AB}^{eff} .

The approaches developed in this manuscript are transferable to a wide range of problems involving active Brownian motion, and the general path-integral framework can be extended to include multipoint statistics. However, this requires inclusion of multiple fixed active-force values within the development to account for the correlations in their impact on the particle statistics. Regardless, the methods developed in this work form the basis for analysis of such effects for arbitrary potentials of interaction. The results for the active Brownian particle in a harmonic potential serve an important role in the study of an active Brownian polymer, and we extend our work to address this problem in a companion work to this manuscript [59]. Furthermore, the impact of environmental heterogeneities [60] and fluctuations [61] on particle and polymer dynamics can be formulated based on our theoretical approach, and we will exploit these connections in future work.

ACKNOWLEDGMENTS

Funding for this work is provided by the Human Frontier Science Program, Grant No. HFSP/REF RGP0019/20.

APPENDIX A: SOLUTION FOR POSITION CORRELATION FROM SPECTRAL DENSITY OF FLUCTUATING FORCES

We provide an alternative derivation of the position-time-correlation function and the corresponding MSD of the particle in the presence of active forces without information about the full probability distribution or steady-state solution. A brief sketch of the derivation of correlation functions in the presence of both thermal and active noise is given below, which matches previously derived results in Ref. [62]. The overdamped Langevin equation in dimensionless units is given as

$$\frac{du(\tau)}{d\tau} = -u(\tau) + F_B(\tau) + F_A(\tau),$$

where

$$\begin{aligned} \langle F_B(\tau_1)F_B(\tau_2) \rangle &= \kappa^{(B)}(\tau_1 - \tau_2) = 2\delta(\tau_1 - \tau_2) \\ \langle F_A(\tau_1)F_A(\tau_2) \rangle &= \kappa^{(A)}(|\tau_1 - \tau_2|) = F_A^2 e^{-K_A(|\tau_1 - \tau_2|)}. \end{aligned}$$

Fourier transformation ($\tau \rightarrow \omega$) of the Langevin equation gives

$$(1 - i\omega)\hat{u}(\omega) = \hat{F}_B(\omega) + \hat{F}_A(\omega).$$

The spectral density is given by

$$\begin{aligned} \hat{S}_u(\omega) &= \frac{\hat{S}_F(\omega)}{|1 - i\omega|^2} = \left(2 + \frac{2F_A^2 K_A}{K_A^2 + \omega^2}\right) \frac{1}{1 + \omega^2} \\ &= \frac{2}{1 + \omega^2} + \frac{2F_A^2 K_A}{(K_A^2 + \omega^2)(1 + \omega^2)}. \end{aligned} \quad (\text{A1})$$

The corresponding time-dependent correlation function can be found from the inverse Fourier transform as

$$\begin{aligned} C_u(\tau) &= \langle u(\tau)u(0) \rangle = \frac{1}{2\pi} \int_{-\infty}^{\infty} d\omega e^{-i\omega\tau} \hat{S}_u(\omega) \\ &= e^{-\tau} + \frac{F_A^2}{K_A^2 - 1} (K_A e^{-\tau} - e^{-K_A\tau}). \end{aligned}$$

This result agrees with Eq. (28) in our manuscript and results from Ref. [62]. Mean-squared displacement of the particle can be calculated using $\text{MSD}(\tau) = \langle [u(\tau) - u(0)]^2 \rangle = 2[C_u(0) - C_u(\tau)]$ as written in Eq. (31).

APPENDIX B: ALTERNATIVE DERIVATION OF THE STEADY-STATE DISTRIBUTION IN EQ. (30)

Following Ref. [48] we propose an alternative way to derive the steady-state distribution in Eq. (30). Positions of a

trapped particle in the presence of Gaussian white and colored noises follow a set of Langevin equations given as

$$\begin{aligned} \dot{u}(\tau) &= -u(\tau) + \sqrt{2}\xi_1(\tau) + F_A(\tau), \\ \dot{F}_A(\tau) &= -K_A F_A(\tau) + \sqrt{2\Gamma} K_A \xi_2(\tau), \end{aligned} \quad (\text{B1})$$

where $\xi_1(\tau)$ and $\xi_2(\tau)$ represent uncorrelated white noise Gaussian processes with zero mean and unit variance. We first write out the Fokker-Planck (FP) operator [48,63] $\hat{\mathcal{L}}$ corresponding to the set of linear equations and for the steady-state solution note $\hat{\mathcal{L}}\mathcal{P}_s(u, F_A) = 0$. The FP operator can be split into several parts involving a pure Ornstein-Uhlenbeck FP generator that follows $\hat{\mathcal{L}}_{\text{OU}}P_n(F_A) = -nP_n(F_A)$, where $P_n(x)$ is the n th-order physicist's Hermite polynomial. The solution to the steady-state distribution involving both variables can be written as a perturbation involving u -dependent series terms and F_A -dependent Hermite polynomials. Going through the process as sketched in Ref. [48], we find

$$\mathcal{P}_s(u, F_A) = \frac{1}{\mathcal{N}} \exp(-\alpha u^2 - \beta F_A^2 + \theta u F_A), \quad (\text{B2})$$

in agreement with Ref. [64]. The exact expressions of the coefficients α , β , and θ can be found from manipulating the expressions given in Ref. [48]. We find the position-dependent steady-state solution to be

$$\begin{aligned} \mathcal{P}_s(u) &= \int_{-\infty}^{\infty} dF_A' \mathcal{P}_s(u, F_A') \\ &= \frac{1}{\mathcal{N}} \exp\left\{-\frac{u^2}{2[1 + \Gamma K_A/(1 + K_A)]}\right\}, \end{aligned} \quad (\text{B3})$$

which matches with Eq. (30).

-
- [1] É. Fodor, C. Nardini, M. E. Cates, J. Tailleur, P. Visco, and F. van Wijland, How Far from Equilibrium Is Active Matter? *Phys. Rev. Lett.* **117**, 038103 (2016).
- [2] E. Flenner and G. Szamel, Active matter: Quantifying the departure from equilibrium, *Phys. Rev. E* **102**, 022607 (2020).
- [3] P. Romanczuk, M. Bär, W. Ebeling, B. Lindner, and L. Schimansky-Geier, Active Brownian particles, *Eur. Phys. J.: Spec. Top.* **202**, 1 (2012).
- [4] A. P. Solon, M. E. Cates, and J. Tailleur, Active Brownian particles and run-and-tumble particles: A comparative study, *Eur. Phys. J.: Spec. Top.* **224**, 1231 (2015).
- [5] J. T. Park, G. Paneru, C. Kwon, S. Granick, and H. K. Pak, Rapid-prototyping a Brownian particle in an active bath, *Soft Matter* **16**, 8122 (2020).
- [6] M. A. Taye, Free energy and entropy production rate for a Brownian particle that walks on overdamped medium, *Phys. Rev. E* **94**, 032111 (2016).
- [7] L. Dabelow, S. Bo, and R. Eichhorn, Irreversibility in Active Matter Systems: Fluctuation Theorem and Mutual Information, *Phys. Rev. X* **9**, 021009 (2019).
- [8] C. Dombrowski, L. Cisneros, S. Chatkaew, R. E. Goldstein, and J. O. Kessler, Self-Concentration and Large-Scale Coherence in Bacterial Dynamics, *Phys. Rev. Lett.* **93**, 098103 (2004).
- [9] J. Elgeti, R. G. Winkler, and G. Gompper, Physics of microswimmers—single particle motion and collective behavior: A review, *Rep. Prog. Phys.* **78**, 056601 (2015).
- [10] S. Das, A. Garg, A. I. Campbell, J. Howse, A. Sen, D. Velegol, R. Golestanian, and S. J. Ebbens, Boundaries can steer active Janus spheres, *Nat. Commun.* **6**, 8999 (2015).
- [11] D. L. Hu, S. Phonekeo, E. Altshuler, and F. Brochard-Wyart, Entangled active matter: From cells to ants, *Eur. Phys. J.: Spec. Top.* **225**, 629 (2016).
- [12] F. Schweitzer, *Brownian Agents and Active Particles: Collective Dynamics in the Natural and Social Sciences* (Springer, Berlin, 2003).
- [13] A. Cavagna and I. Giardina, Bird flocks as condensed matter, *Annu. Rev. Condens. Matter Phys.* **5**, 183 (2014).
- [14] C. Bechinger, R. Di Leonardo, H. Löwen, C. Reichardt, G. Volpe, and G. Volpe, Active particles in complex and crowded environments, *Rev. Mod. Phys.* **88**, 045006 (2016).
- [15] K. E. S. Tang and K. A. Dill, Native protein fluctuations: The conformational-motion temperature and the inverse correlation of protein flexibility with protein stability, *J. Biomol. Struct. Dyn.* **16**, 397 (1998).

- [16] M. B. Elowitz, A. J. Levine, E. D. Siggia, and P. S. Swain, Stochastic gene expression in a single cell, *Science* **297**, 1183 (2002).
- [17] P. S. Swain, M. B. Elowitz, and E. D. Siggia, Intrinsic and extrinsic contributions to stochasticity in gene expression, *Proc. Natl. Acad. Sci. USA* **99**, 12795 (2002).
- [18] S. Christoforidis, H. M. McBride, R. D. Burgoyne, and M. Zerial, The Rab5 effector EEA1 is a core component of endosome docking, *Nature (London)* **397**, 621 (1999).
- [19] D. H. Murray, M. Jahnel, J. Lauer, M. J. Avellaneda, N. Brouilly, A. Cezanne, H. Morales-Navarrete, E. D. Perini, C. Ferguson, A. N. Lupas *et al.*, An endosomal tether undergoes an entropic collapse to bring vesicles together, *Nature (London)* **537**, 107 (2016).
- [20] M. D. ElAlaoui Faris, D. Lacoste, J. Pécéréaux, J.-F. Joanny, J. Prost, and P. Bassereau, Membrane Tension Lowering Induced by Protein Activity, *Phys. Rev. Lett.* **102**, 038102 (2009).
- [21] P. A. Janmey and P. K. J. Kinnunen, Biophysical properties of lipids and dynamic membranes, *Trends Cell Biol.* **16**, 538 (2006).
- [22] P. Bassereau and P. Sens, *Physics of Biological Membranes* (Springer, Berlin, 2018).
- [23] H. Turlier and T. Betz, Unveiling the active nature of living-membrane fluctuations and mechanics, *Annu. Rev. Condens. Matter Phys.* **10**, 213 (2019).
- [24] G. H. Koenderink, Z. Dogic, F. Nakamura, P. M. Bendix, F. C. MacKintosh, J. H. Hartwig, T. P. Stossel, and D. A. Weitz, An active biopolymer network controlled by molecular motors, *Proc. Natl. Acad. Sci. USA* **106**, 15192 (2009).
- [25] D. Mizuno, C. Tardin, C. F. Schmidt, and F. C. MacKintosh, Nonequilibrium mechanics of active cytoskeletal networks, *Science* **315**, 370 (2007).
- [26] P. A. Pullarkat, P. A. Fernández, and A. Ott, Rheological properties of the eukaryotic cell cytoskeleton, *Phys. Rep.* **449**, 29 (2007).
- [27] M. Doi and S. F. Edwards, *The Theory of Polymer Dynamics* International Series of Monographs on Physics Vol. 73 (Oxford University, Oxford, England, 1988).
- [28] S. C. Weber, A. J. Spakowitz, and J. A. Theriot, Nonthermal ATP-dependent fluctuations contribute to the in vivo motion of chromosomal loci, *Proc. Natl. Acad. Sci. USA* **109**, 7338 (2012).
- [29] A. Zidovska, D. A. Weitz, and T. J. Mitchison, Micron-scale coherence in interphase chromatin dynamics, *Proc. Natl. Acad. Sci. USA* **110**, 15555 (2013).
- [30] F.-Y. Chu, S. C. Haley, and A. Zidovska, On the origin of shape fluctuations of the cell nucleus, *Proc. Natl. Acad. Sci. USA* **114**, 10338 (2017).
- [31] C. M. Caragine, S. C. Haley, and A. Zidovska, Surface Fluctuations and Coalescence of Nucleolar Droplets in the Human Cell Nucleus, *Phys. Rev. Lett.* **121**, 148101 (2018).
- [32] P. Girard, J. Prost, and P. Bassereau, Passive or Active Fluctuations in Membranes Containing Proteins, *Phys. Rev. Lett.* **94**, 088102 (2005).
- [33] V. Levi, Q. Ruan, M. Plutz, A. S. Belmont, and E. Gratton, Chromatin dynamics in interphase cells revealed by tracking in a two-photon excitation microscope, *Biophys. J.* **89**, 4275 (2005).
- [34] I. Bronstein, Y. Israel, E. Kepten, S. Mai, Y. Shav-Tal, E. Barkai, and Y. Garini, Transient Anomalous Diffusion of Telomeres in the Nucleus of Mammalian Cells, *Phys. Rev. Lett.* **103**, 018102 (2009).
- [35] A. Javer, N. J. Kuwada, Z. Long, V. G. Benza, K. D. Dorfman, P. A. Wiggins, P. Cicuta, and M. C. Lagomarsino, Persistent super-diffusive motion of *Escherichia coli* chromosomal loci, *Nat. Commun.* **5**, 3854 (2014).
- [36] T. Sakaue and T. Saito, Active diffusion of model chromosomal loci driven by athermal noise, *Soft Matter* **13**, 81 (2017).
- [37] A. Einstein, On the theory of the Brownian movement, *Ann. Phys.* **19**, 371 (1906).
- [38] M. Smoluchowski, The kinetic theory of Brownian molecular motion and suspensions, *Ann. Phys.* **21**, 756 (1906).
- [39] É. Fodor and M. E. Cates, Active engines: Thermodynamics moves forward, *Europhys. Lett.* **134**, 10003 (2021).
- [40] T. Speck, Stochastic thermodynamics for active matter, *Europhys. Lett.* **114**, 30006 (2016).
- [41] T. Markovich, É. Fodor, E. Tjhung, and M. E. Cates, Thermodynamics of Active Field Theories: Energetic Cost of Coupling to Reservoirs, *Phys. Rev. X* **11**, 021057 (2021).
- [42] A. P. Solon, J. Stenhammar, M. E. Cates, Y. Kafri, and J. Tailleur, Generalized thermodynamics of motility-induced phase separation: Phase equilibria, laplace pressure, and change of ensembles, *New J. Phys.* **20**, 075001 (2018).
- [43] A. J. McKane, Noise-induced escape rate over a potential barrier: Results for general noise, *Phys. Rev. A* **40**, 4050 (1989).
- [44] P. Hänggi and P. Jung, Colored noise in dynamical systems, *Adv. Chem. Phys.* **89**, 239 (1995).
- [45] R. Wittmann, C. Maggi, A. Sharma, A. Scacchi, J. M. Brader, and U. M. B. Marconi, Effective equilibrium states in the colored-noise model for active matter. I. Pairwise forces in the fox and unified colored noise approximations, *J. Stat. Mech.: Theory Exp.* (2017) 113207.
- [46] R. Wittmann, U. M. B. Marconi, C. Maggi, and J. M. Brader, Effective equilibrium states in the colored-noise model for active matter. II. A unified framework for phase equilibria, structure and mechanical properties, *J. Stat. Mech.: Theory Exp.* (2017) 113208.
- [47] S. Ramaswamy, Active matter, *J. Stat. Mech.: Theory Exp.* (2017) 054002.
- [48] D. Martin and T. A. de Pirey, AOUP in the presence of Brownian noise: A perturbative approach, *J. Stat. Mech.: Theory Exp.* (2021) 043205.
- [49] L. P. Dadhichi, A. Maitra, and S. Ramaswamy, Origins and diagnostics of the nonequilibrium character of active systems, *J. Stat. Mech.: Theory Exp.* (2018) 123201.
- [50] L. Dabelow and R. Eichhorn, Irreversibility in active matter: General framework for active Ornstein-Uhlenbeck particles, *Front. Phys.* **8**, 582992 (2021).
- [51] A. M. Menzel, On the way of classifying new states of active matter, *New J. Phys.* **18**, 071001 (2016).
- [52] S. Dal Cengio, D. Levis, and I. Pagonabarraga, Linear Response Theory and Green-Kubo Relations for Active Matter, *Phys. Rev. Lett.* **123**, 238003 (2019).
- [53] M. E. Cates and J. Tailleur, Motility-induced phase separation, *Annu. Rev. Condens. Matter Phys.* **6**, 219 (2015).
- [54] A. P. Solon, J. Stenhammar, R. Wittkowski, M. Kardar, Y. Kafri, M. E. Cates, and J. Tailleur, Pressure and Phase Equilibria

- in Interacting Active Brownian Spheres, *Phys. Rev. Lett.* **114**, 198301 (2015).
- [55] L. Caprini, A. Puglisi, and A. Sarracino, Fluctuation–dissipation relations in active matter systems, *Symmetry* **13**, 81 (2021).
- [56] S. Dal Cengio, D. Levis, and I. Pagonabarraga, Fluctuation–dissipation relations in the absence of detailed balance: formalism and applications to active matter, *J. Stat. Mech.: Theory Exp.* (2021) 043201.
- [57] J. L. Doob, The Brownian movement and stochastic equations, *Ann. Math.* **43**, 351 (1942).
- [58] G. A. Pavliotis, *Stochastic Processes and Applications: Diffusion Processes, the Fokker-Planck and Langevin equations*, Texts in Applied Mathematics Vol. 60 (Springer, Berlin, 2014).
- [59] A. Ghosh and A. J. Spakowitz, Interplay of active and thermal fluctuations in non-equilibrium and living biological systems, (to be published).
- [60] A. J. Spakowitz, Transient anomalous diffusion in a heterogeneous environment, *Front. Phys.* **7**, 119 (2019).
- [61] P. C. Cai, B. A. Krajina, and A. J. Spakowitz, Brachiation of a polymer chain in the presence of a dynamic network, *Phys. Rev. E* **102**, 020501(R) (2020).
- [62] D. Osmanović and Y. Rabin, Dynamics of active Rouse chains, *Soft Matter* **13**, 963 (2017).
- [63] L. L. Bonilla, Active Ornstein-Uhlenbeck particles, *Phys. Rev. E* **100**, 022601 (2019).
- [64] G. Szamel, Self-propelled particle in an external potential: Existence of an effective temperature, *Phys. Rev. E* **90**, 012111 (2014).